INTERNATIONAL JOURNAL OF AUTOMOTIVE AND MECHANICAL ENGINEERING (IJAME)
ISSN: 2229-8649 e-ISSN: 2180-1606
VOL. 19, ISSUE 1, 9487 – 9497
DOI: https://doi.org/10.15282/ijame.19.1.2022.12.0731

ORIGINAL ARTICLE

Modeling of Crashworthiness criteria based on Variation of Hole as Crush Initiator in Thin-Walled Square

F. Dionisius[1,2,*], J. Istiyanto[2], D. A. Sumarsono[2], G. Prayogo[2], A. S. Baskoro[2] and M. Malawat[3]

[1]Department of Mechanical Engineering, Politeknik Negeri Indramayu, 45252 West Java, Indonesia
[2]Department of Mechanical Engineering, Faculty of Engineering, Universitas Indonesia, 16424 West Java, Indonesia
[3]Department of Transportation, Maluku Provincial Government, 97117 Ambon, Indonesia

ABSTRACT – Crashworthiness is the ability to protect its occupant by absorbing the energy of impact during a collision. A crush initiator is one way to increase crashworthiness criteria at collision. The most widely applied crush initiator applications are holes, wall thickness reduction, grooves, notch, bead and corrugated. This study discussed making a functional model from the crashworthiness criteria which is known by CFE and SEA. Variable used variations of the crush initiator in the form of circular holes with different rotation angles and diameters. The rotation angle referred to in this study was 2 holes which are rotated based on the midpoint of the hole distance to the radial axis of the hole. The crush initiator was placed in a square column at each side with steel material. Besides, the wall thickness variable was added which can increase the energy absorption during a collision. The method used numerical simulation and experimental dynamic loading. The numerical simulation used the explicit finite element method by using ESI PAM-Crash. Both methods used the drop test model by using impact transferability. Impact transferability was rigid which was used to transfer impact loading during impact conditions. Experimental was used to validate the function model which was obtained through the least square method with sampling from numerical simulations. The results showed the same patterns produced by the functional and experimental models using the Taguchi method (L9) with 3 runs. The maximum of this pattern is 23% for CFE and 17% for SEA. Meanwhile, the average error of the S/N ratio shows 8.77% for CFE and 2.16% for SEA. This model function could be used by a crashworthy designer to estimate the value of CFE and SEA.

ARTICLE HISTORY
Received: 1st July 2021
Revised: 5th Feb 2022
Accepted: 1st Mar 2022

KEYWORDS
Model function;
Crush initiator;
Crashworthiness;
Taguchi method;
Least square method

INTRODUCTION

The application of thin-walled structure is widely used in the world of automotive, shipping, aviation, and construction because of lightweight and also economical. In the automotive world, this structure is often used for energy absorption when the collision occurred [1], [2] which is known as crashworthiness. To reduce the impact of injuries on passengers, the peak crushing force (P_{max}), crush force efficiency (CFE), and specific energy absorption (SEA) were investigated. A way to overcome this problem in the automotive world is the crumple zone, especially if the collision happens from the front by placing a thin-walled structure known as the front rail. The front rail can absorb 40% of kinetic energy during impact collision [3], [4]. Researchers were investigating many ways to optimize thin-walled structures by crush initiators. It could change the crashworthiness criteria to be optimal as well as utilization in local bending arrangements through crush initiator or trigger of bending.

A crush initiator with general imperfection in the column was used for the transition process which results in the phenomenon of the general buckling process to progressive buckling. This had been investigated by Abramowicz and Jones [5]. A roll-wrapped tube with a crush initiator had been analyzed by Browne et al [6]. The front rail on the vehicle was analyzed by providing hole type and dent type crush nucleator which was done by Cho et al [7] with giving axial load. Explicit computation with the help of ANSYS/LS-DYNA was also carried out by Eren et al [8]. It was done by analyzing the rib type initiator. Buckling initiator gave to the upper circular tube and the square tube was analyzed by Zhang et al [9] to obtain peak impact and energy absorption during axial loads. The simulation method with ANSYS/LS-DYNA was carried out by Gumruk et al [10] by using a semi-circular trigger design to obtain peak impact loads and energy absorption that occurred. Similarly, Hussain et al [11]–[13] used triggers to increase energy absorption by using numerical simulation and experimental method. The type of trigger was made by front-end trigger and slot trigger on GFRP specimens with square, cylindrical, hexagonal, and decagonal cross-sections. The test was carried out using the LS-DYNA for numerical simulation method. In contrast to Tong et al [14], who investigated the cylindrical tube using an external trigger. This external trigger was a molding that has a semi-circle cavity and a chamfer. This test was carried out with numerical and experimental simulations under dynamic loading conditions. Chen et al [15] also used molding as an initiator with different models of CFRP materials, with different layups of U and W models. This initiator increased SEA from both quasi-static and dynamic loading.

*CORRESPONDING AUTHOR | Felix Dionisius | ✉ felix.dionisius@polindra.ac.id

Istiyanto et al [3] also investigated and compared the use of circular hole-shaped tubes between non-crush initiators by numerical simulation and experimental quasi-static. Similar to Subramaniyan et al [16] who conducted square and circular tubes by giving circular holes to get energy absorption. Li et al [17] had done an optimization of the multiobjective design of square tube containing foam with the surrogate model method. Abbasi et al [18] also optimized multi-angle designs using the experimental orthogonal array design introduced by Taguchi. Likewise, Sun et al [19] had done optimization with robust design algorithms that use the Taguchi method on the geometry of tailed welded tubes related to crashworthiness criteria.

Estrada et al. [20] investigated energy absorption (EA) and crush force efficiency (CFE) by using cross-sections (circular shape, rectangle, and polygon), bi-tubular clearance, and holes as variables in specimens. The specimens had aluminum 6063-T5 which was used in Johnson-Cook (J-C) model by using the finite element method. It showed that CFE could increase by using a circular shape and increasing clearance. While holes could increase EA and CFE. Pirmohammad and Marzdashti [21] experimented by using finite element analysis LS-DYNA code. Hole of shape, dimension of shape, and bi-tubal structures were examined to get crashworthiness performance as specific energy absorption (SEA) and peak crush force (PCF). The hexagonal shape improved crashworthiness performance which is the biggest SEA dan lowest PCF.

Initiator also was investigated by Nia et al [22] who was in the form cutting on the square tube under oblique loading in quasi-static. It decreased peak crush force but increased crush force efficiency by transforming general buckling to progressive buckling. Malawat et al [23] [24] also investigated the hole position of crush initiator in a square tube by experimentally and theoretically method with quasi dynamic loading. The initiator could decrease the peak loading force. Furthermore, it also increased specific energy absorption. Dionisius et al [25] used a pyramid arrangement of crush initiators to reduce maximum impact force under quasi-static loading. Likewise, Zahran et al [26] used the hole as a crush initiator. The specimen was modified by a tailor-made technique. The specimens were made to resemble a multi-stage square but with different lengths and cutting. Silva et al [27] also conducted an assessment of circular holes in square aluminum and steel with quasi-static loading. The circular hole is installed laterally on the specimen. Sankar et al [28], who conducted crashworthiness on cylinder specimens, The specimens were given circular holes as crush initiators and arranged from single row to multi-stage rows. Rogala et al [29] made a model of peak crush force and total efficiency using the ANN method. Box specimens are given to the initiator or trigger in a hexagonal shape with a position placed close to the fixed support. Peixinho et al. [30] made the initiator with localizing heating in the specimen as a thermal trigger. The specimen used aluminum square 6061-T5 with quasi-static and dynamic loading. It presented high energy absorption and reduced maximum load. Eyvazian et al [31] experimented by using corrugated as buckling initiator on circular metal tubes. The experiment used quasi-static loading in experimentally and theoretically method. It shows that was perfect energy absorption and reducing initial peak load.

Feli et al [32] investigated the conical tube by giving grooved on the wall structure. The tube had given impact loading by analytical and simulation methods. The research resulted in decreasing the initial peak load and energy absorption. Wang et al [33] modified the specimen by following the tibia bone model with a quadrangular cross-section. The specimen was given a groove model as the initiator and an inner core with a negative Poisson's ratio (NPR) model. This study used AMGA and NSGA-II to obtain an increase in energy absorption and effective crashworthiness. Huang and Wang [34] introduced a new trigger which is called a crown trigger. It could reduce the peak load at carbon-fibre-reinforced polymer tubes. Chambe et al. [35] also investigated composite materials with variations in the fiber direction of the layers. The direction of the fiber is used as a trigger to get the ability of SEA in quasi-static loading. Li et al. [36] also used the type and number of crush initiators to increase energy absorption under different angle loading.

Zhou et al [37] conducted a quasi-static test on the tube by adding an initiator in the form of a rectangular window and a slotted window. These initiators were arranged in a row along the tube. The test showed a decrease in the maximum impact force based on an increase in the area ratio between the window and conventional tube. Yuan et al. [38] and Ye et al. [39] also investigated tube specimens with the origami concept, which were pre-folded first. The specimens are square, rectangular, polygonal, and tapered with brass and composite material. The results showed an increase in energy absorption and a decrease in initial peak force.

The above researcher used a pattern of crush initiator which was placed at the prediction hinge of buckling initiation. Buckling initiation could be through crush initiator and corrugated model. The buckling initiation applied in the above study experienced a fold where the crush initiator and corrugated models were arranged according to the perpendicular to the specimen axis. One application of crush initiator is a circular hole which was the variable in this paper due to the easy manufacturing process, using only a drilling machine. In the application, these holes are placed on the vehicle frame randomly, especially the front rail area as shown in Figure 1. It can be seen that the pair of holes is not perpendicular to the axis of the frame.

Based on the existing literature and the application of crush initiators on vehicles, this paper studied the crush initiator which was unplaced at its hinge of buckling by rotating crush initiator. This study used 2 circular holes as crush initiators. The rotation angle was the value of the midline between the two initiators to the line perpendicular to the axial load direction. Furthermore, the wall thickness of the specimen and the diameter of the crush initiator were used in this paper. This experiment was especially important in crashworthiness design where a large number of irregular holes position are applied to the frame. To make it easier for designers, a model function was made to find out the value of crashworthiness, especially CFE and SEA. This modeling had also been carried out by Liu et al [40] who used wall thickness and cross-section variables but did not investigate the crush initiator as one of the variables in the crashworthiness test.

(a) left side frame (b) right side frame

Figure 1. Hole position in a car.

METHODS

Crashworthiness Criteria

Crashworthiness criteria in thin-walled columns are energy absorption (EA), specific energy absorption (SEA), and crush force efficiency (CFE). To get CFE, the average of impact force (P_{mean}) was divided by the maximum impact force (P_{max}). These criteria were referred to Eqs. (1) to (4).

$$EA\ (\Delta) = \int_0^{\Delta} P(\Delta) \tag{1}$$

$$SEA\ (\Delta) = \frac{EA\ (\Delta)}{mass}. \tag{2}$$

$$P_{mean}(\Delta) = \frac{EA(\Delta)}{\Delta}. \tag{3}$$

$$CFE = \frac{P_{mean}(\Delta)}{P_{max}} x\ 100\%. \tag{4}$$

where Δ is total crash displacement and F (Δ) is a function of the impact force on displacement. CFE indicator shows the uniformity of consistency of a given burden [17] where the highest was expected to 100%.

Explicit Finite Element Method

This research used a numerical simulation solution with the help of the PAM-Crash code [4] which used the finite element method concept. Geometry modelling was done with the help of the Visual Mesh with a surface model (see Figure 2) which were impact transferability, specimen (square column), and impactor. Specimen had 36.5×36.5×200 mm in dimension. The specimens had a pair of circular holes on each side of the specimens. The holes were rotated about the horizontal axis by 0°, 45°, and 90° as shown in Figure 3. Besides, the diameter of holes was one of the variables in this research. Impact transferability has two plates and three solid cylinders. The plates are 100 mm in diameter and 20 mm in thickness while the solid cylinder is 50 mm in diameter and 500 mm in length. Both of them were rigid bodies. Elements model was used by Visual Mesh with Belytschko-Tsay of the shell.

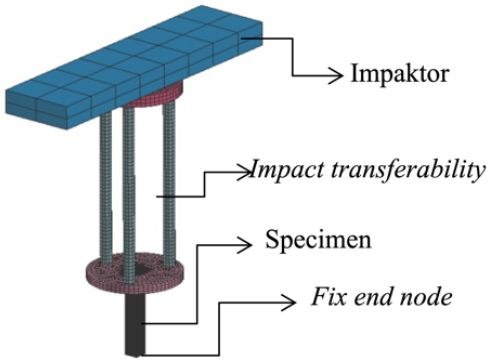

Figure 2. Model of FEM

The square column was modeled by using 2 mm in meshing size with a thickness of 0.6-1 mm. Mechanical properties of square column especially stress-strain was achieved from the tensile test as shown in Figure 4. The material was low carbon steel. The stress-strain was modeled in FEM as data of properties material in elastic-plastic type (104). The

impactor was modeled as a rigid body with 80 kg in mass and 100 mm in meshing size. The initial velocity of the impactor was 5.47 mm/ms which was the start of a collision on the surface of impact transferability. Contact between the square column themselves used 36-type segment with contact distances according to the thickness of the specimen with 0.5 friction coefficient. Square column and impact transferability used 34-type segment to segment with a contact distance of 1 mm with 0.5 in friction coefficient.

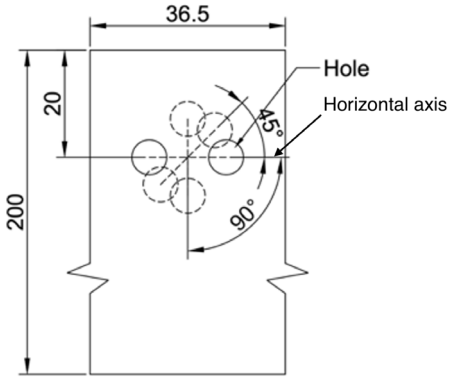

Figure 3. Hole geometry specimens.

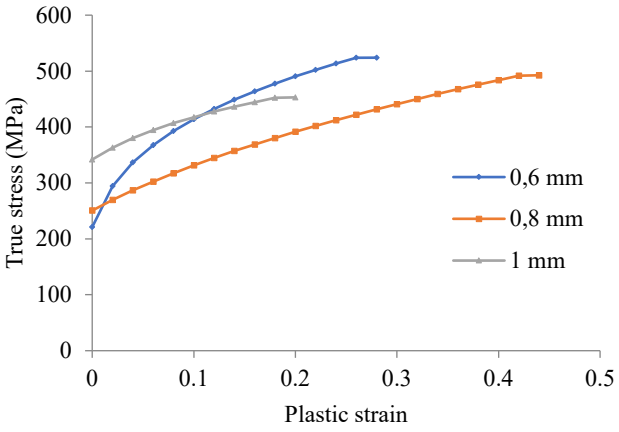

Figure 4. Mechanical properties of specimens.

Least Square Method

In the design process, several methods were used to achieve variables that had a significant effect [40]. The least-square method was built to get the model from 3 variables which are rotation angle (α) of crush initiator, thickness (t) of specimens, and diameter (ϕ) of crush initiator. The response of this criteria was built by referring to Eq. (5).

$$\hat{y}(x) = CFE(\alpha,t,\phi) = \sum_{i=1}^{n} \beta_i \varphi_i(\alpha,t,\phi) \tag{5}$$

Which n represents the total number of basic functions, $\varphi_i(\alpha,t,\phi)$. In this research, polynomial was used to produce a basic function to get the model of crashworthiness criteria (CFE and SEA). B_i is regression coefficient in this method.

The yielded response, y_i $(y_1 - y_m)$ was produced by observation of sampling design m (m>n). After that, least-square function (L) was made that is referred to Eq.(6). ε_i is the error between the response y_i.

$$\mathrm{L} = \sum_{i=1}^{m} \epsilon_i^2 = \sum_{i=1}^{m} \left[y_i - \sum_{j=1}^{n} \beta_i \varphi_i(\alpha,t,\phi) \right]^2 \tag{6}$$

Coefficient vector $b = (\beta_1, \beta_2, \ldots, \beta_n)$ could be determined by the derivative of $\partial L/\partial \beta = 0$ in referring to Eqs. (7) and (8),

$$b = (\phi^T \phi)^1 \phi^T y \tag{7}$$

$$\phi = \begin{bmatrix} \varphi_1(\alpha,t,\phi)_1 & \cdots & \varphi_n(\alpha,t,\phi)_1 \\ \cdots & \cdots & \cdots \\ \varphi_1(\alpha,t,\phi)_m & \cdots & \varphi_n(\alpha,t,\phi)_m \end{bmatrix} \tag{8}$$

New model function (SEA and CFE) was produced by substituting Eqs. (8) into (5). The function could be evaluated by the coefficient of determination, R^2, which are calculated by referring to Eqs. (9)-(11). R^2 is a statistical measure that represents the proportion of total sum of squares (SS_T) by the residual sum of squares (SS_E).

$$SS_E = \sum_{i=1}^{m} (y_i - \hat{y}_i)^2 \tag{9}$$

$$SS_T = \sum_{i=1}^{m} (y_i - \bar{y}_i)^2 \tag{10}$$

$$R^2 = 1 - \frac{SS_E}{SS_T} \tag{11}$$

Which, $\hat{y}_i$ is original response at i and $\bar{y}_i$ is the mean value of y_i

Experimental Method

The experimental method used the concept of drop test where an 80 kg of the impactor with 1,5 m in height from the surface of impact transferability. The impactor would drop and hit the surface of impact transferability as in Figure 5. The photodiode was set up as a trigger at the camera when hit the surface of impact transferability and starting of recording the load cell. This camera had 1000 fps in capacities. The specimen was placed in impact transferability as a vertical position. This method would produce the graph of displacement-force with load cell PCB Piezoelectric 203B with 88.96 kN in capacities. Variation of experimental used Taguchi Method with 2 tools which are signal-noise ratio and orthogonal array.

Figure 5. Experimental method

S/N Ratio

Taguchi method described several methods in solving the effect of the contribution of each variable by using the signal to noise (S/N) ratio. S/N ratio was used to measure quality characteristics in the. desired value. This ratio used the priority of the results achieved to measure a characteristic of the desired value with an uncontrollable factor which is noise. To measure the characteristic in this research, the mathematical function was referred to Eqs. (12) and (13) [41]. For example, in terms of crashworthiness criteria, the high of CFE and SEA was the best option.

$$S/N = -10 \log MSD \tag{12}$$

$$\text{MSD} = \frac{\frac{1}{Y_i^2}}{n} \tag{13}$$

where MSD is the mean square deviation, Y_i is the value of the experimental combination and n number of experimental repetitions.

Orthogonal Array

The Taguchi method can significantly minimize the experimental cost and testing time using an orthogonal array. This orthogonal array used 3 variables which are rotation angle (α), the thickness (t), and the diameter of the crush initiator (ϕ). To simplify the definition of the condition of the specimen at the time of testing, label A was as rotation angle, B as wall thickness, and C as the diameter of the crush initiator. Each variable of specimens had 3 levels as shown in Table 1. The orthogonal array used inner array dan outer array with 9 combinations (L9) as Table 2. So that the definition of condition $A_1B_1C_1$ was a square column, which has the first level for rotation angle, thickness, and diameter of crush initiator. Furthermore, $A_3B_3C_2$ was the third level for rotation angle, thickness, the second level in the diameter. To get a good S/N ratio, several repeating observation was done 3 repetitions (R_1-R_3).

Table 1. Variables in the experiment.

Variables / Levels	α (°)	t (mm)	ϕ (mm)
1	0	0.6	3
2	45	0.8	6.5
3	90	1	10

Table 2. Inner and outer of an orthogonal array (L9).

Design	Inner array			Outer array		
	Level			SEA or CFE		
	α (°)	t (mm)	ϕ (mm)	R_1	R_2	R_3
$A_1B_1C_1$	1	1	1	…	…	…
$A_1B_2C_2$	1	2	2	…	…	…
$A_1B_3C_3$	1	3	3	…	…	…
$A_2B_1C_2$	2	1	2	…	…	…
$A_2B_2C_3$	2	2	3	…	…	…
$A_2B_3C_1$	2	3	1	…	…	…
$A_3B_1C_3$	3	1	3	…	…	…
$A_3B_2C_1$	3	2	1	…	…	…
$A_3B_3C_2$	3	3	2	…	…	…

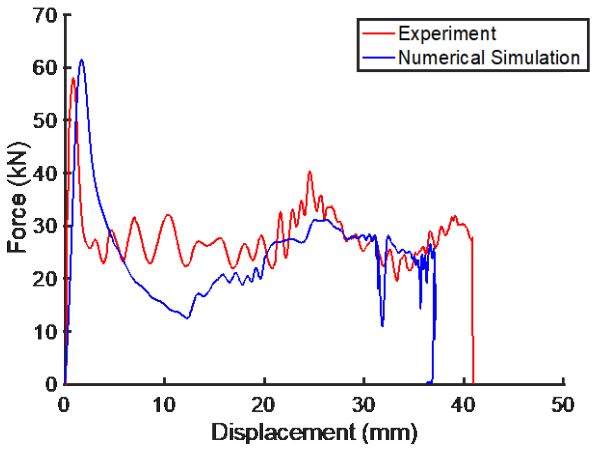

Figure 6. Displacement-force graph.

RESULTS AND DISCUSSION

The numerical simulation used the explicit finite element method with full factorial of experiment which is 27 conditions. The method produced a graph of displacement and force (see Figure 6) which were used to analyze the crashworthiness criteria by referring to Eqs.(1) to (4). The results could be seen in Table 3. Specimens underwent initial progressive buckling in the hole for 0° and 45° and 90°, as shown in Figure 7. This shows that even though the hole was

rotated about the horizontal axis, initial progressive buckling would be experienced at the hole closest to the initial impact surface.

Table 3. CFE and SEA in numerical simulation

No.	α (°)	t (mm)	ϕ (mm)	CFE (%)	SEA (J/kg)
1	0	0.6	3	25.82	7167.77
2	0	0.6	6.5	24.84	7199.36
3	0	0.6	10	26.38	7213.47
4	0	0.8	3	32.69	5038.44
5	0	0.8	6.5	28.05	5152.36
6	0	0.8	10	25.30	5244.55
7	0	1	3	37.46	4268.58
8	0	1	6.5	36.56	4495.92
9	0	1	10	36.74	4347.24
10	45	0.6	3	24.12	7160.63
11	45	0.6	6.5	24.42	7197.83
12	45	0.6	10	26.79	7322.66
13	45	0.8	3	30.33	5109.05
14	45	0.8	6.5	29.98	5255.98
15	45	0.8	10	33.47	5295.46
16	45	1	3	38.92	4190.53
17	45	1	6.5	38.22	4353.15
18	45	1	10	38.58	4273.43
19	90	0.6	3	26.84	7097.74
20	90	0.6	6.5	25.71	7170.62
21	90	0.6	10	24.91	7124.87
22	90	0.8	3	32.47	5099.09
23	90	0.8	6.5	30.51	5246.24
24	90	0.8	10	25.59	5267.25
25	90	1	3	36.28	4418.43
26	90	1	6.5	35.46	4322.59
27	90	1	10	34.73	4565.59

Table 3 was processed into a quadratic polynomial function by making the variables α, t, ϕ, α^2, αt, αϕ, t^2, tϕ, ϕ^2. The making of this variable was based on reference [40]. From these results, the CFE and SEA functions were referred to Eqs. (15) and (16). Refer to Eq. (11), two functions had R^2 which was 0.90 for CFE and 0.99 for SEA.

$$CFE\ (\alpha, t, \phi) = 28.024 + 0.100\alpha - 24.093t - 0.341\phi - 0.001\alpha^2 - 0.043\alpha t - 0.001\alpha\phi + 36.084t^2 - 0.467t\phi + 0.045\phi^2 \quad (15)$$

$$SEA\ (\alpha, t, \phi) = 20111.331 - 2.947\alpha - 30551.986t + 44.602\phi + 0.003\alpha^2 + 3.539\alpha t + 0.006\alpha\phi + 14546.623t^2 + 8.793t\phi - 2.646\phi^2 \quad (16)$$

The function model above could show that in the significant effect lies the wall thickness in obtaining CFE and SEA. Meanwhile, the diameter and angle of rotation were not significant compared to the wall thickness in the specimens. This was revealed by Djamaluddin et al. [42] and Kuznetcov et al. [43] which could reduce SEA if the wall thickness was increased. But from these two variables (diameter and angle rotation), the effect of diameter was greater than the angle of rotation in obtaining CFE and SEA. The diameter would affect the length of the hinge line. The length of this line would repeatedly change the wavelength, which changes the average of impact force (P_{mean}). To produce the maximum impact force (P_{max}), the diameter could also affect the stress concentration factor. A larger diameter would decrease the stress concentration factor which results in a decrease in the maximum impact force [24], [44]. The two factors would affect the CFE. If seen in Figure 7, every buckling prefix always occurred in the hole so that the factor for determining CFE and SEA had an insignificant value.

Equations (15) and (16) would be validated experimentally with the Taguchi method which was shown in Table 2. This experiment also produced force and displacement graphs (see Figure 6) and initial buckling (see Figure 7). In general, crashworthiness tests would experience progressive buckling of the structure. Progressive buckling in real-time also did not experience significant differences between simulation and experimental for all specimens. For example, it could be seen in the $A_3B_2C_1$ specimen (see Figure 9) which was full folded 5 times and half-folded 1 time in the final stage. The figure shows that the displacement has no difference between numerical simulation and experimental. This image also strengthens the graph in Figure 6.

This experimental method was carried out in 3 runs. The error of data of this experiment used impact maximum force (P_{max}) and mean force (P_{mean}) as shown in Figure 8. Based on this figure, it could be seen that only $A_3B_3C_2$ had the highest error in P_{max} and P_{mean}. Meanwhile, the P_{max} and P_{mean} show the same pattern. This show that the data is still acceptable

for processing into CFE and SEA. CFE and SEA would be known through its equation by entering the three variables which are rotation angle, wall thickness, and diameter of crush initiators. Results of the equation and experimental could be seen in Figure 10. Results of the experiment and functions model show the same pattern in which between designs experience fluctuating values. Comparing the two methods, CFE and SEA have a maximum error value of 23% and 17% which is located in the designs of $A_3B_2C_1$ dan $A_2B_2C_3$.

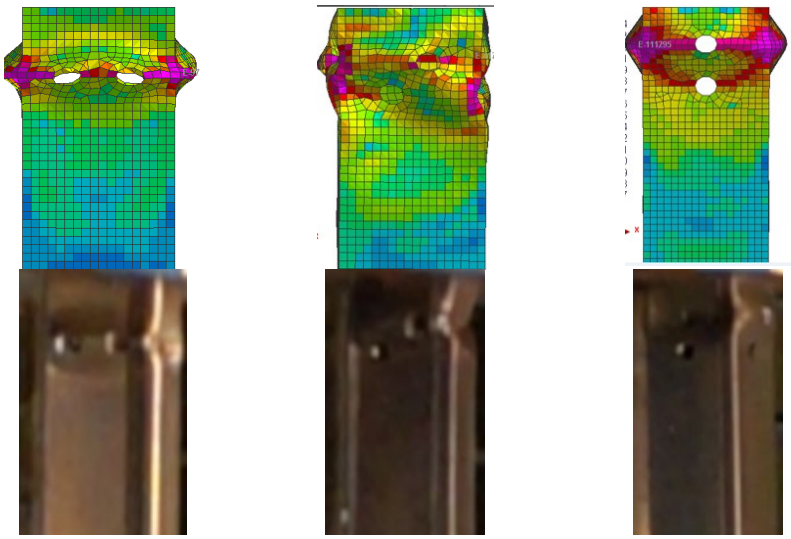

(a) angle 0° (b) angle 45° (c) angle 90°

Figure 7. Initial buckling

To measure the characteristic level of this value (experiment and function), the S/N ratio value is referred to Eq. (12). The S/N ratio in the experiment used repetition n = 3 because the experiment was carried out using 3 repetitions for one condition (design). Meanwhile, the function model only used n = 1. The results between the experiment and the function model can be seen in Table 4. The experimental and model function had 8.77% and 2.16% in the error of the S/N ratio.

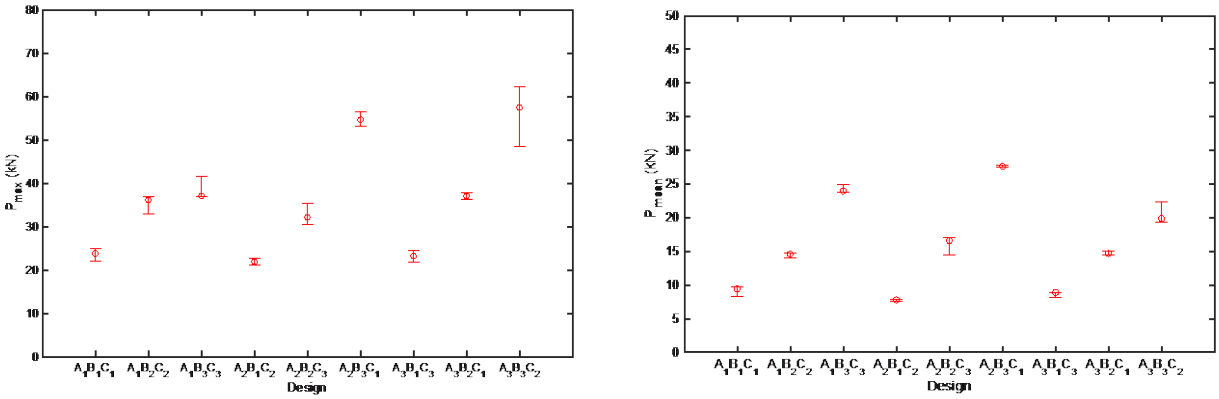

(a) P_{max} (b) P_{mean}

Figure 8. Error bar.

Table 4. S/N ratio.

Design	S/N CFE		S/N SEA	
	Experiment	Function	Experiment	Function
$A_1B_1C_1$	31.17	27.99	80.14	77.08
$A_1B_2C_2$	32.24	29.28	75.35	74.33
$A_1B_3C_3$	35.29	31.23	72.69	72.82
$A_2B_1C_2$	31.09	28.31	78.34	77.15
$A_2B_2C_3$	33.24	29.59	76.76	74.38
$A_2B_3C_1$	34.02	31.83	75.37	72.62
$A_3B_1C_3$	31.33	27.96	78.58	77.16
$A_3B_2C_1$	31.95	29.66	76.25	74.20
$A_3B_3C_2$	32.28	31.06	74.06	72.92
$\overline{S/N}$	32.51	29.66	76.39	74.74
Error $\overline{S/N}$	8.77%		2.16%	

In order to make the function more valid, the data above would be compared with experiments that have been carried out by other researchers. The compared data were CFE and SEA data with the crush initiator at a position of 20 mm and a rotation angle of 0°. The data is shown in Table 5. CFE only used a comparison of 0.8 mm thickness while SEA was only 0.6 and 1 mm in thickness. The CFE was directly taken from the experimental results, while the SEA was processed through the distribution of the EA in the article with the mass of this paper such as Eq. (2). The error shown in the table shows a difference of 13% for CFE. Meanwhile, there was a significant difference in SEA where the thickness of 0.6 and 1 mm is 9% and 29%, respectively. This difference was caused by differences in the mechanical properties of the material such as yield strength and tensile strength. In addition, the material used in the numerical simulation is a true stress-strain. Meanwhile, other experiments in Table 5 used engineering stress-strain. The results of this comparison indicated that an increase in wall thickness would reduce SEA. When compared with Liu et al [40], there were differences in SEA trends related to the wall thickness variable. This was due to the same mechanical properties in the numerical simulation modeling. Meanwhile, in this study, the tensile test results (see Figure 4) were used for numerical simulation modeling.

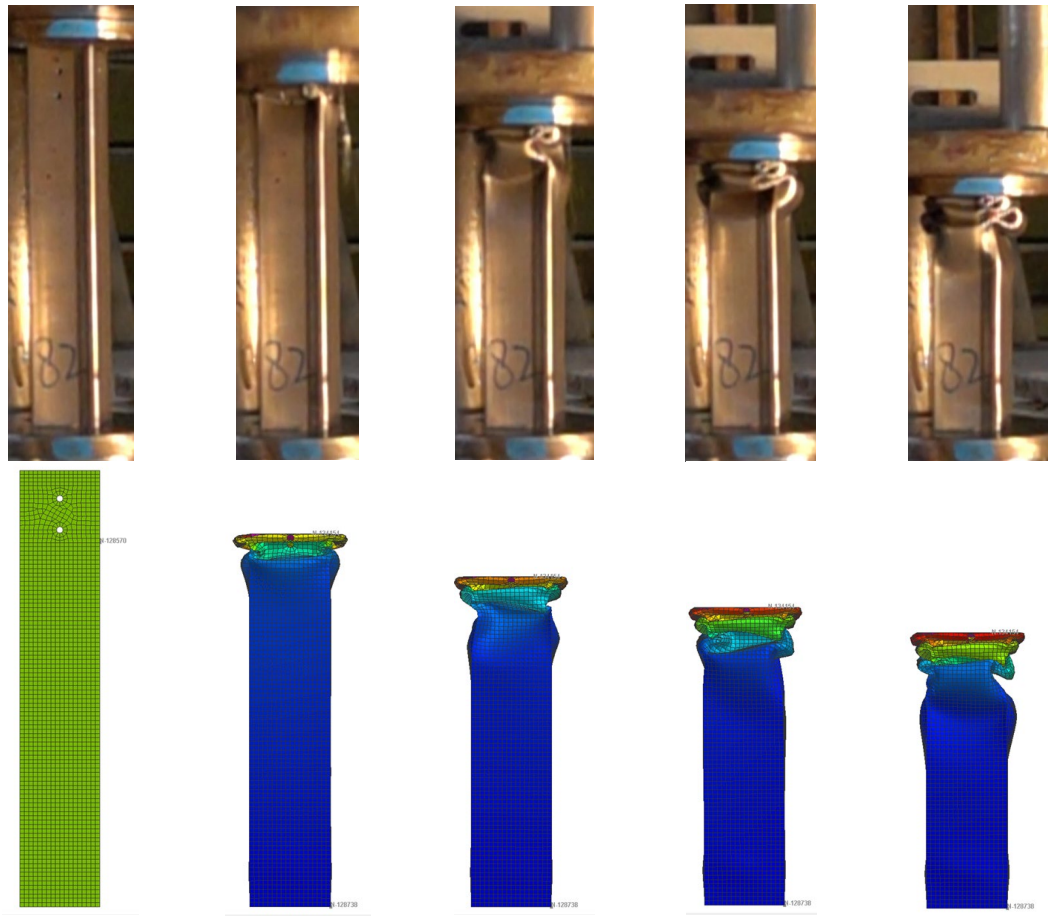

Figure 9. Progressive buckling in $A_3B_2C_1$ (90° in rotation angle, 0.8 mm in thickness, 6.5 mm in diameter)

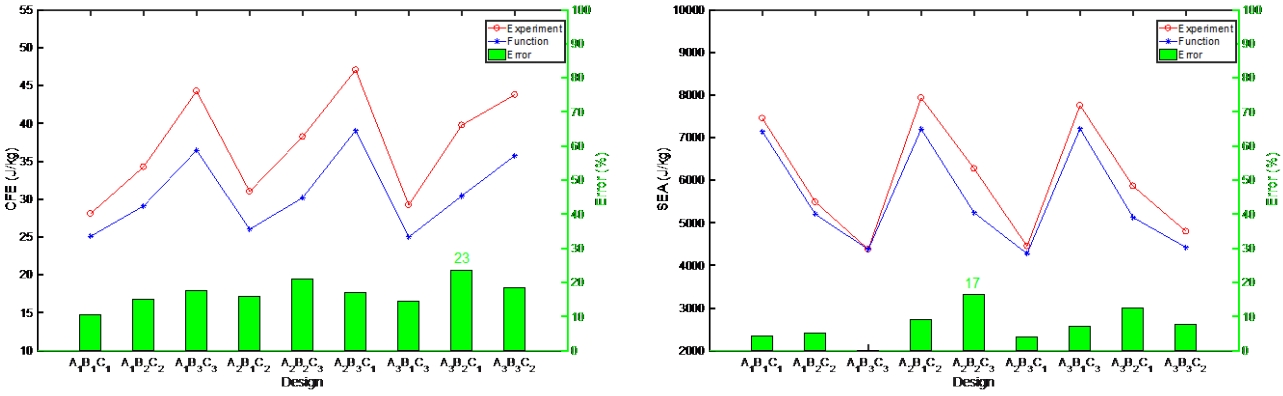

(a) CFE (b) SEA

Figure 10. Comparing criteria in experiment and functional model.

Table 5. Comparing in other experiment for variation thickness

α (°)	t (mm)	ϕ (mm)	Function of Eq. (15) and (16)		Other experiments		Error (%)	
			CFE (%)	SEA(J)	CFE (%)	SEA* (J)	CFE	SEA
0	0.6	6.5	-	7229	-	5592 [23]	-	29
	0.8		29.09	-	33[45]	-	13	-
	1		-	4341	-	3985 [23]	-	9

Note: * processed by Eq. (2)

CONCLUSION

The impact test on the thin-walled square had been carried out using numerical simulation methods. These specimens had variations in wall thickness and crush initiator in the form of holes with variations in rotation angle and diameter. The function model had also been generated through the least square method based on the data from the numerical simulation results. The validation of the function model was carried out by experiment using the Taguchi method. The graph between the experiments and the functional model has the same pattern with a maximum error of 23% for CFE and 17% for SEA. Meanwhile, the average S/N ratio between the experiment and the functional model had a maximum error of 8.77% for CFE and 2.16% for SEA. This function model can be applied as a prefix to find the best SEA and CFE before carrying out a crash test on a vehicle. In the future, further research is needed regarding the creation of a function model if the crush initiator is located in any place of the square structure.

ACKNOWLEDGEMENT

This work supported by Departemen Riset dan Pengabdian Masyarakat Universitas Indonesia by Hibah Riset Pascasarjana, Indonesia.

REFERENCES

[1] W. Abramowicz, "Thin-walled structures as impact energy absorbers," *Thin-Walled Struct.*, vol. 41, pp. 91–107, 2003, doi: 10.1016/S0263-8231(02)00082-4.

[2] F. Tarlochan *et al.*, "Design of thin wall structures for energy absorption applications: Enhancement of crashworthiness due to axial and oblique impact forces," *Thin-Walled Struct.*, vol. 71, pp. 7–17, 2013, doi: 10.1016/j.tws.2013.04.003.

[3] J. Istiyanto *et al.*, "Experiment and numerical study – Effects of crush initiators under quasi-static axial load of thin wall square tube," *Appl. Mech. Mater.*, vol. 660, pp. 628–632, 2014, doi: 10.4028/www.scientific.net/AMM.660.628.

[4] G. Balaji and K. Annamalai, "An experimental and numerical scrutiny of crashworthiness variables for square column with V-notch and groove initiators under quasi-static loading," *Cogent Eng.*, vol. 4, pp. 1–20, 2017, doi: 10.1080/23311916.2017.1364118.

[5] W. Abramowicz and N. Jones, "Transition from initial global bending to progressive buckling of tubes loaded statically and dynamically," *Int. J. Impact Eng.*, vol. 19, no. 5–6, pp. 415–437, 1997, doi: 10.1016/s0734-743x(96)00052-8.

[6] A. L. Browne and N. L. Johnson, "Dynamic axial crush tests of roll wrapped composite tubes: plug vs. non-plug crush initiators," in *Proceedings of IMECE2005*, 2005, pp. 1–9.

[7] Y. B. Cho, C. H. Bae, M. W. Suh, and H. C. Sin, "A vehicle front frame crash design optimization using hole-type and dent-type crush initiator," *Thin-Walled Struct.*, vol. 44, no. 4, pp. 415–428, 2006, doi: 10.1016/j.tws.2006.03.011.

[8] I. Eren, Y. Gür, and Z. Aksoy, "Finite element analysis of collapse of front side rails with new types of crush initiators," *Int. J. Automot. Technol.*, vol. 10, no. 4, pp. 451–457, 2009, doi: 10.1007/s12239.

[9] X. W. Zhang, Q. D. Tian, and T. X. Yu, "Axial crushing of circular tubes with buckling initiators," *Thin-Walled Struct.*, vol. 47, no. 6–7, pp. 788–797, 2009, doi: 10.1016/j.tws.2009.01.002.

[10] R. Gümrük and S. Karadeniz, "A numerical study of the influence of bump type triggers on the axial crushing of top hat thin-walled sections," *Thin-Walled Struct.*, vol. 46, no. 10, pp. 1094–1106, 2008, doi: 10.1016/j.tws.2008.01.031.

[11] N. Nasir Hussain, S. Prakash Regalla, and Y. V. Daseswara Rao, "Low velocity impact characterization of glass fiber reinforced plastics for application of crash box," in *Materials Today: Proceedings*, 2017, vol. 4, no. 2, pp. 3252–3262, doi: 10.1016/j.matpr.2017.02.211.

[12] N. N. Hussain, S. P. Regalla, and V. D. Rao Yendluri, "Numerical investigation into the effect of various trigger configurations on crashworthiness of GFRP crash boxes made of different types of cross sections," *Int. J. Crashworthiness*, vol. 22, no. 5, pp. 565–581, 2017, doi: 10.1080/13588265.2017.1286964.

[13] N. N. Hussain, S. P. Regalla, Y. V. D. Rao, and A. M. Mohammed, "An experimental and numerical analysis on influence of triggering for composite automotive crash boxes under compressive impact loads," *Int. J. Crashworthiness*, pp. 1–15, May 2021, doi: 10.1080/13588265.2021.1914953.

[14] Y. Tong and Y. Xu, "Improvement of crash energy absorption of 2D braided composite tubes through an innovative chamfer external triggers," *Int. J. Impact Eng.*, vol. 111, pp. 11–20, 2018, doi: 10.1016/j.ijimpeng.2017.08.002.

[15] Y. Chen, L. Ye, J. P. Escobedo-Diaz, and Y. X. Zhang, "Effect of initiator geometry on energy absorption of CFRP tubes under dynamic crushing," *Int. J. Crashworthiness*, vol. 26, no. 5, pp. 526–536, 2021, doi: 10.1080/13588265.2020.1761585.

[16] S. K. Subramaniyan *et al.*, "Crush characteristics and energy absorption of thin-walled tubes with through-hole crush initiators," *Appl. Mech. Mater.*, vol. 606, pp. 181–185, 2014, doi: 10.4028/www.scientific.net/AMM.606.181.

[17] F. Li, G. Sun, X. Huang, J. Rong, and Q. Li, "Multiobjective robust optimization for crashworthiness design of foam filled thin-walled structures with random and interval uncertainties," *Eng. Struct.*, vol. 88, pp. 111–124, 2015, doi: 10.1016/j.engstruct.2015.01.023.

[18] M. Abbasi, S. Reddy, A. Ghafari-Nazari, and M. Fard, "Multiobjective crashworthiness optimization of multi-cornered thin-walled sheet metal members," *Thin-Walled Struct.*, vol. 89, pp. 31–41, 2015, doi: 10.1016/j.tws.2014.12.009.

[19] G. Sun *et al.*, "Discrete robust optimization algorithm based on Taguchi method for structural crashworthiness design," *Expert Syst. Appl.*, vol. 42, no. 9, pp. 4482–4492, 2015, doi: 10.1016/j.eswa.2014.12.054.
[20] Q. Estrada *et al.*, "Effect of radial clearance and holes as crush initiators on the crashworthiness performance of bi-tubular profiles," *Thin-Walled Struct.*, vol. 140, pp. 43–59, 2019, doi: 10.1016/j.tws.2019.02.039.
[21] S. Pirmohammad and S. Esmaeili-Marzdashti, "Multi-objective crashworthiness optimization of square and octagonal bitubal structures including different hole shapes," *Thin-Walled Struct.*, vol. 139, pp. 126–138, 2019, doi: 10.1016/j.tws.2019.03.004.
[22] A. Alavi Nia, K. Fallah Nejad, H. Badnava, and H. R. Farhoudi, "Effects of buckling initiators on mechanical behavior of thin-walled square tubes subjected to oblique loading," *Thin-Walled Struct.*, vol. 59, pp. 87–96, 2012, doi: 10.1016/j.tws.2012.03.002.
[23] M. Malawat, J. Istiyanto, and D. A. Sumarsono, "Effects of wall thickness and crush initiators position under experimental drop test on square tubes," *Appl. Mech. Mater.*, vol. 865, pp. 612–618, 2017, doi: 10.4028/www.scientific.net/amm.865.612.
[24] M. Malawat *et al.*, "Theoretical prediction of dynamic axial crushing on a square tube with eight holes used as a crush initiator," *Int. J. Technol.*, vol. 10, no. 5, pp. 1042–1055, 2019, doi: 10.1017/CBO9781107415324.004.
[25] F. Dionisius *et al.*, "An increase in crashworthiness capability using pyramid arrangement of the crush initiator," in *IOP Conf. Series: Materials Science and Engineering 850*, 2020, p. 012049, doi: 10.1088/1757-899X/850/1/012049.
[26] M. S. Zahran, P. Xue, M. S. Esa, and M. M. Abdelwahab, "A novel tailor-made technique for enhancing the crashworthiness by multi-stage tubular square tubes," *Thin-Walled Struct.*, vol. 122, no. 2018, pp. 64–82, 2018, doi: 10.1016/j.tws.2017.09.031.
[27] R. de C. Silva, J. C. de S. Teles, and A. B. de S. Oliveira, "Experimental and numerical performance assessment of square aluminum and steel energy absorbers with circular hole discontinuities," *Int. J. Crashworthiness*, vol. 0, no. 0, pp. 1–17, 2021, doi: 10.1080/13588265.2021.1906511.
[28] H. Ravi Sankar and V. Parameswaran, "Effect of circular perforations on the progressive collapse of circular cylinders under axial impact," *Int. J. Impact Eng.*, vol. 122, pp. 346–362, 2018, doi: 10.1016/j.ijimpeng.2018.09.001.
[29] M. Rogala, J. Gajewski, and M. Górecki, "Study on the effect of geometrical parameters of a hexagonal trigger on energy absorber performance using ann," *Materials (Basel).*, vol. 14, no. 20, 2021, doi: 10.3390/ma14205981.
[30] N. Peixinho *et al.*, "Experimental study of impact energy absorption in aluminium square tubes with thermal triggers," *Mater. Res.*, vol. 15, no. 2, pp. 323–332, 2012, doi: 10.1590/S1516-14392012005000011.
[31] A. Eyvazian, T. N. Tran, and A. M. Hamouda, "Experimental and theoretical studies on axially crushed corrugated metal tubes," *Int. J. Non. Linear. Mech.*, vol. 101, pp. 86–94, 2018, doi: 10.1016/j.ijnonlinmec.2018.02.009.
[32] S. Feli, E. Makhsousse, and S. S. Jafari, "Dynamic progressive buckling of thin-wall grooved conical tubes under impact loading," *Int. J. Crashworthiness*, vol. 0, no. 0, pp. 1–10, 2019, doi: 10.1080/13588265.2019.1573476.
[33] C. Y. Wang *et al.*, "Structure design and multi-objective optimization of a novel crash box based on biomimetic structure," *Int. J. Mech. Sci.*, vol. 138–139, pp. 489–501, 2018, doi: 10.1016/j.ijmecsci.2018.01.032.
[34] J. Huang and X. Wang, "On a new crush trigger for energy absorption of composite tubes," *Int. J. Crashworthiness*, vol. 15, no. 6, pp. 625–634, 2010, doi: 10.1080/13588265.2010.484194.
[35] J. E. Chambe *et al.*, "Effects of dynamics and trigger on energy absorption of composite tubes during axial crushing," *Int. J. Crashworthiness*, vol. 26, no. 5, pp. 549–567, 2021, doi: 10.1080/13588265.2020.1766175.
[36] Z. Li, S. Rakheja, and W. Bin Shangguan, "Study on crushing behaviors of foam-filled thin-walled square tubes with different types and number of initiators under multiple angle loads," *Thin-Walled Struct.*, vol. 145, no. August, p. 106376, 2019, doi: 10.1016/j.tws.2019.106376.
[37] C. Zhou *et al.*, "The energy absorption of rectangular and slotted windowed tubes under axial crushing," *Int. J. Mech. Sci.*, vol. 141, pp. 89–100, 2018, doi: 10.1016/j.ijmecsci.2018.03.036.
[38] L. Yuan, H. Shi, J. Ma, and Z. You, "Quasi-static impact of origami crash boxes with various profiles," *Thin-Walled Struct.*, vol. 141, no. March, pp. 435–446, 2019, doi: 10.1016/j.tws.2019.04.028.
[39] H. Ye *et al.*, "Energy absorption behaviors of pre-folded composite tubes with the full-diamond origami patterns," *Compos. Struct.*, vol. 221, p. 110904, 2019, doi: 10.1016/j.compstruct.2019.110904.
[40] Y. Liu, "Optimum design of straight thin-walled box section beams for crashworthiness analysis," *Finite Elem. Anal. Des.*, vol. 44, no. 3, pp. 139–147, 2008, doi: 10.1016/j.finel.2007.11.003.
[41] R. K. Roy, *Design of experiments using the taguchi approach*. New York: John Wiley & Sons, Inc, 2001.
[42] F. Djamaluddin, S. Abdullah, A. K. Ariffin, and Z. M. Nopiah, "Finite element analysis and crashworthiness optimization of foam-filled double circular under oblique loading," *Lat. Am. J. Solids Struct.*, vol. 13, no. 11, pp. 2176–2189, 2016, doi: 10.1590/1679-78252844.
[43] A. Kuznetcov, I. Telichev, and C. Q. Wu, "Effect of thin-walled tube geometry on its crashworthiness performance," in *International LS-DYNA Users Conference*, 2016, pp. 1–12.
[44] C. N. Nguyen, T. Dirgantara, L. Gunawan, and H. A. Ly, "Analytical prediction of square crash box," in *Regional Conference on Mechanical and Aerospace Technology*, 2013, no. November, pp. 1–10, doi: 10.13140/2.1.4896.8642.
[45] A. S. Danardono, M. Malawat, and J. Istiyanto, "Pengembangan impact energy absorber dengan pengaturan jarak crash initiator (development of impact energy absorber with distance management of crash initiators)," in *Proceeding Seminar Nasional Tahunan Teknik Mesin*, 2015, no. SNTTM XIV, p. MT-15.